UNIVERSIDADE FEDERAL DO RIO GRANDE DO SUL
Seminário do Programa de Pós-Graduação em Engenharia Química

OKTOBER FÓRUM 2005 – PPGEQ 10 anos

NMPC WITH STATE-SPACE MODELS OBTAINED THROUGH LINEARIZATION ON EQUILIBRIUM MANIFOLD

Stephan Koch, Ricardo G. Duraiski, Pedro B. Fernandes, Jorge O. Trierweiler

Group of Integration, Modelling, Simulation, Control and Optimization of Processes (GIMSCOP)
Department of Chemical Engineering, Universidade Federal do Rio Grande do Sul (UFRGS).
Rua Luiz Englert, s/n, ZIP CODE: 90040-040, Porto Alegre - RS - Brazil.
{stephan, ricardo, pedro, jorge}*@enq.ufrgs.br*

Abstract: This paper presents a Nonlinear Model Predictive Control approach for nonlinear state-space models obtained with the modelling and identification technique recently proposed in literature as Linearization on the Equilibrium Manifold (LEM). The predictive controller that will be applied to the LEM uses the Local Linearization on the Trajectory algorithm (LLT) which simulates the nonlinear plant and calculates optimal control actions based on local linearizations around the simulated trajectory by online minimization of an objective function. The proposed combination of the LEM and LLT techniques is tested with two nonlinear SISO systems.

Keywords: nonlinear systems, identification, linearization, predictive control, trajectories

1. INTRODUCTION

The importance of nonlinear approaches to control systems in industrial chemical processes has been rising significantly during the last few years and will continue to do so in the future. The high demands of today's economy in terms of process yield and the obedience of environmental standards require an increased efficiency that cannot always be achieved with linear control concepts. At the same time, the availability of nonlinear dynamic models has been recognized in the literature as one of the main obstacles, if not the most important, for the application of nonlinear control strategies. High cost and complexity of nonlinear approaches often impose restrictions on practical usability.

This situation calls for methods that take into account the well-developed linear control theory, extending it for usage with nonlinear processes. One possibility, which can be termed "grey-box" modelling, is the use of "local models", understood as approximations of the original system in a limited sub-region of the operating domain in order to construct a nonlinear model. The underlying principle is that the system behavior is "simpler" locally than globally and as a result local models can be identified more easily. Examples of this methodology are the local linear models tree (Nelles, 1997) and the identification through the decomposition into operating regimes (Johansen and Murray-Smith, 1997).

The Linearization on the Equilibrium Manifold (LEM) approach (Fernandes and Engell, 2005) proposes a different way of constructing a nonlinear model by interpolating the equilibrium manifold and the linear behavior of the system between different operating points. It has been shown that various problems of local modelling techniques can be avoided by using this method, making it an appealing way of obtaining a nonlinear model.
A suitable control strategy for this kind of system would also use linear models for determining control actions, as these are already available and in use for the construction of the global model. The Local Linearization on the Trajectory algorithm LLT (Duraiski, 2001) is a predictive control strategy for nonlinear models which uses local linearizations at the current point of the system state. In the following, a combination with of the LLT with LEM models will be proposed.

This paper is structured as follows: section 2 presents the basics of the LEM method, section 3 explains the LLT control strategy. Section 4 proposes a combination of the two isolated methods, which is evaluated in numerical experiments in section 5. Concluding remarks and proposals for further investigations can be found in Section 6.

2. LINEARIZATION ON THE EQUILIBRIUM MANIFOLD (LEM) MODELS

Consider a continuous SISO nonlinear dynamic system of the form

$$\begin{aligned}\dot{\mathbf{x}} &= \mathbf{r}(\mathbf{x},\mathbf{u}) \\ \mathbf{y} &= \mathbf{h}(\mathbf{x})\end{aligned} \qquad (1)$$

where $\mathbf{r}$: $X \times U \rightarrow \Re^n$ is at least once continuously differentiable on $X \subseteq \Re^n$, $U \subseteq \Re^m$, and $\mathbf{h}$: $X \rightarrow \Re^p$ is at least once continuously differentiable. The output equation will be frequently omitted in the sequel for shortness. The equilibrium manifold of (1) is defined as the family of constant equilibrium points

$$\Xi = \left\{ (\mathbf{x}_s, \mathbf{u}_s, \mathbf{y}_s) \in \Re^n \times \Re^n \times \Re^n : \; \mathbf{r}(\mathbf{x}_s, \mathbf{u}_s) = \mathbf{0}, \; \mathbf{y}_s = \mathbf{h}(\mathbf{x}_s, \mathbf{u}_s) \right\}. \qquad (2)$$

Similarly, the family of linearizations of (1) at the set of equilibrium points determined by (2) is given is in the usual way as

$$\dot{\mathbf{x}} = \left[\frac{\partial \mathbf{r}(\mathbf{x},\mathbf{u})}{\partial \mathbf{x}} \right]_{\mathbf{x}_s,\mathbf{u}_s} (\mathbf{x} - \mathbf{x}_s) + \left[\frac{\partial \mathbf{r}(\mathbf{x},\mathbf{u})}{\partial \mathbf{u}} \right]_{\mathbf{x}_s,\mathbf{u}_s} (\mathbf{u} - \mathbf{u}_s) \qquad (3)$$

and similarly for the output equation. Under the condition that the rank of $[\partial \mathbf{r}(\mathbf{x}_s,\mathbf{u}_s)/\partial \mathbf{x}]$ is n for the set Ξ (Wang and Rugh, 1987, Fernandes 2005), the equilibrium manifold and consequently the family of linearizations of (1) will be specified by m among the $n + m$ variables $(\mathbf{x},\mathbf{u})$. Therefore, if this matrix is full rank, the set of inputs fully parameterize both families of equilibrium points and linearizations.

Calling the steady-state map $\mathbf{\Omega}$: $\Re^m \rightarrow \Re^n$, such that $\mathbf{r}(\mathbf{\Omega}(\mathbf{u}),\mathbf{u}) = \mathbf{0}$ (that is, the function $\mathbf{\Omega}$ gives the steady-state $\mathbf{x}_s$ corresponding to a constant input $\mathbf{u}_s$), the input-parameterized linearization around the equilibrium manifold (LEM) of (1) is defined as the system (Fernandes 2005, Fernandes and Engell, 2005)

$$\dot{\mathbf{x}} = \mathbf{A}(\mathbf{u})(\mathbf{x} - \mathbf{\Omega}(\mathbf{u})) \qquad (4)$$

$\mathbf{A}(\mathbf{u})$ represents the evaluation of the Jacobian matrix $[\partial \mathbf{r}(\mathbf{x},\mathbf{u})/\partial \mathbf{x}]$ on $(\mathbf{\Omega}(\mathbf{u}),\mathbf{u})$. The focus on input parameterization is due to the fact that identification experiments are carried out by exciting the plant with a designed input signal. The output equation can be linearized in an analogous way, considering the stationary output mapping: $\mathbf{\Psi}$: $\Re^m \rightarrow \Re^p$.

The model (4) has to be interpreted as *a* (state-affine) nonlinear system that possesses the same family of equilibrium points (2) and the same linearization family (4) as the nonlinear system (1). Following the discussion in (Fernandes, 2005), the LEM system can constitute also a good approximation of (1) in transient regimes away from the equilibrium manifold, depending on its "degree" of nonlinearity. Obviously, other representations that are equivalent on the equilibrium manifold can be constructed on the basis of any m distinct parameters. Moreover, these representations can be easily interchanged, provided that the inverses of the corresponding elements in $\mathbf{\Omega}(\mathbf{u})$ and $(\mathbf{u})$ exist. For further information about how to obtain the equilibrium manifold and the dynamic matrix $\mathbf{A}$, please refer to Fernandes (2005).

3. LOCAL LINERIZATIONS ON THE TRAJECTORY (LLT)

In the following section a control strategy for the model introduced above will be presented. It was developed by Duraiski (2001) and consists of a model predictive control algorithm which works in the following way: the control actions applied to the manipulated variables are obtained by optimizing an objective function of control costs using a nonlinear internal model to predict the future system outputs. The control actions, however, are determined in each iteration through the use of a set of linear models in the step response form, obtained through local linearizations around the trajectory of the system, previously obtained in the last iteration. This ensures that the optimization problem is quadratic as it is in the case of Linear Model Predictive Control, and thus easy to solve.

3.1 Algorithm description

The LLT algorithm (Duraiski, 2001) consists of the following iterative calculation steps:

1) The first solution is based on a linearized model at the current operating conditions. Using this trajectory it is possible to simulate the nonlinear model which is used to calculate a sequence of linear models for the next iteration.
2) With the sequence of linearized models on the trajectory a new control action trajectory is calculated.
3) This sequence of control moves is applied to the simulation of the open-loop response of the internal model.
4) Based on the new trajectory, it is possible to determine a new set of linearized models in the same way as it is done in the first step. Then, this set of models is used in the next iteration step.
5) The steps 2, 3 and 4 are sequentially carried out until the algorithm converges, i.e., when the last two trajectories do not differ too much to each other considering a given norm.

3.2 Linearized Step Response Model

In this part the linear step response model used for calculating control actions will be developed. We consider the discrete time state space equation

$$(\mathbf{x}_k - \mathbf{x}^B_{k-1}) = \mathbf{A}_{k-2} \cdot (\mathbf{x}_{k-1} - \mathbf{x}^B_{k-2}) + \mathbf{B}_{k-2} \cdot (\mathbf{u}_{k-1} - \mathbf{u}^B_{k-2}) \quad (5)$$

$$(\mathbf{y}_k - \mathbf{y}^B_{k-1}) = \mathbf{C}_{k-1} \cdot (\mathbf{x}_k - \mathbf{x}^B_{k-1}) + \mathbf{D}_{k-1} \cdot (\mathbf{u}_k - \mathbf{u}^B_{k-1}) \quad (6)$$

The matrices $\mathbf{A}_{k-2}$, $\mathbf{B}_{k-2}$, $\mathbf{C}_{k-1}$ and $\mathbf{D}_{k-1}$ are obtained by *discretization* of the continuous linear state space system resulting from the Taylor linearization of equation (1). They are not to be confused with the traditional notation for the continuous state space matrices (i.e., **A**, **B**, **C** and **D)**. The variables $\mathbf{x}^B$, $\mathbf{u}^B$, $\mathbf{y}^B$ represent the variables **x**, **u**, **y** at the point of linearization. Equations (5) and (6) can now be applied iteratively for the time steps from 0 up to the control horizon P, yielding an output equation for each discrete step time. With this, an equation for the output **Y** from the time instant 0 to P can be constructed. Written in a compact matrix form, the following equation is obtained:

$$\mathbf{Y}_{\left[\begin{smallmatrix}P\\0\end{smallmatrix}\right]} = \mathbf{Su} \cdot \boldsymbol{\delta}\mathbf{U}_{\left[\begin{smallmatrix}P\\0\end{smallmatrix}\right]} + \mathbf{Sx} \cdot \boldsymbol{\delta}\mathbf{x}_0 + \mathbf{Y}^B_{\left[\begin{smallmatrix}P-1\\-1\end{smallmatrix}\right]} \quad (7)$$

Equation (7) will be used with some alterations within the calculation and optimization of the objective function. For details please refer to Duraiski (2001).

3.3 Objective function

The optimization problem consists of the minimization of a quadratic objective function with penalty terms for setpoint deviations and control actions, in the most general form being

$$J = \min_{\Delta U_{\left[\begin{smallmatrix}M\\0\end{smallmatrix}\right]}} \left(\sum_{i=0}^{P} (\gamma_i \cdot (y_i - r_i))^2 + \sum_{i=0}^{M} (\lambda_i \cdot \Delta u_i)^2 \right) \quad (8)$$

In the case of the LLT method, the input difference variable $\Delta u_k = u_k - u_{k-1}$ is replaced by the deviation variable $\delta u_k = u_k - u_{k-1}{}^B$. Furthermore, a penalty term for soft constraints $\varphi|s|$ and for the deviation of the manipulated variable from a given target z_i are introduced. With these alterations, the objective function for the optimization problem is

$$J = \min_{\delta U_{\left[\begin{smallmatrix}M\\0\end{smallmatrix}\right]}} \begin{pmatrix} \sum_{i=0}^{P} (\gamma_i \cdot (y_i - r_i))^2 + \\ \sum_{i=0}^{M} \left(\lambda_i \cdot \left((\delta u_i + u^B_{i-1}) - (\delta u_{i-1} + u^B_{i-2})\right)\right)^2 + \\ \sum_{i=0}^{M} \left(\psi_i \cdot \left((\delta u_i + u^B_{i-1}) - z_i\right)\right)^2 + (\varphi|s|)^2 \end{pmatrix} \quad (9)$$

For implementation, equation (9) can be rewritten in a matrix form. Further details will not be discussed here and can be found in (Duraiski, 2001).

4. COMBINING A LEM MODEL WITH AN LLT CONTROLLER

Now a combination of models obtained through the LEM technique with a nonlinear model predictive controller using the LLT method will be proposed. In general, two possibilities exist to achieve this goal: first, using the LEM as a nonlinear model for the LLT algorithm as it is, deriving the needed Jacobians **A**, **B**, **C**, **D** through analytic or numerical differentiation of the LEM itself. A second possible approach is altering the LLT algorithm in a way that it can deal directly with the dynamic matrix **A** and the stationary manifold vector $\boldsymbol{\Omega}(\mathbf{u})$ of the LEM. In this work only the first possibility will be investigated, as it demonstrates the feasibility of the approach with fairly low effort in terms of implementation. The control performance and computational effort of the LEM+LLT combination will be compared to an LLT controller with a nonlinear model.

It will be assumed in the sequel that a nonlinear LEM model in the autonomous state space form as stated in equation (4) has been constructed by identifying the matrix **A** and the equilibrium manifold $\boldsymbol{\Omega}(\mathbf{u})$ using appropriate techniques. Further details about model construction can be found in (Fernandes, 2005). Equation (4) will now be the incorporated into the LLT algorithm, using it as a description of the nonlinear process. As can be seen in equations (5) and (6), it is necessary to derive a general linearization of the process for later discretization and the calculation of control actions by the LLT. This is achieved by a straight-forward Taylor linearization of the LEM model around an arbitrary point ($\mathbf{x}^B$, $\mathbf{u}^B$) in state space. Note that this has to be a dynamic linearization as we cannot assume the system to be at an equilibrium state at all times. However, the resulting *bias* caused by the term $\mathbf{r}(\mathbf{x}^B, \mathbf{u}^B) = \mathbf{A}(\mathbf{u}^B)(\mathbf{x}^B - \boldsymbol{\Omega}(\mathbf{u}^B))$ will cancel out in the differential equation, as shown in (Duraiski, 2001, Appendix B).

Linearizing equation (4) around an arbitrary point ($\mathbf{x}^B$,$\mathbf{u}^B$) in state space yields:

$$\begin{aligned} \Delta\dot{\mathbf{x}} &= \left.\frac{\partial(\mathbf{r}(\mathbf{x},\mathbf{u})}{\partial\mathbf{x}}\right|_{\mathbf{x}^B\mathbf{u}^B} \cdot \Delta\mathbf{x} + \left.\frac{\partial(\mathbf{r}(\mathbf{x},\mathbf{u}))}{\partial\mathbf{u}}\right|_{\mathbf{x}^B\mathbf{u}^B} \cdot \Delta\mathbf{u} \\ &= \mathbf{A}(\mathbf{u}^B)\Delta\mathbf{x} + \left.\frac{\partial\mathbf{A}(\mathbf{u})}{\partial\mathbf{u}}\right|_{\mathbf{u}^B} \cdot \mathbf{x}^B \cdot \Delta\mathbf{u} \\ &\quad - \left.\frac{\partial\mathbf{A}(\mathbf{u})}{\partial\mathbf{u}}\right|_{\mathbf{u}^B} \cdot \boldsymbol{\Omega}(\mathbf{u}^B) \cdot \Delta\mathbf{u} - \mathbf{A}(\mathbf{u}^B) \cdot \left.\frac{\partial\boldsymbol{\Omega}(\mathbf{u})}{\partial\mathbf{u}}\right|_{\mathbf{u}^B} \Delta\mathbf{u} \end{aligned} \quad (10)$$

With this the following matrixes are obtained:

$$\mathbf{A}^B = \mathbf{A}(\mathbf{u}^B)$$
$$\mathbf{B}^B = \frac{\partial \mathbf{A}(\mathbf{u})}{\partial \mathbf{u}}\Big|_{\mathbf{u}^B} \cdot \left(\mathbf{x}^B - \boldsymbol{\Omega}(\mathbf{u}^B)\right) - \mathbf{A}(\mathbf{u}^B) \cdot \frac{\partial \boldsymbol{\Omega}(\mathbf{u})}{\partial \mathbf{u}}\Big|_{\mathbf{u}^B} \quad (11)$$

The output equation from (1) can also be linearized in a straight-forward way, yielding matrices $\mathbf{C}^B$ and $\mathbf{D}^B$ for the linear state space model.

$$\Delta \mathbf{y} = \frac{\partial (\mathbf{h}(\mathbf{x}))}{\partial \mathbf{x}}\Big|_{\mathbf{x}^B} \cdot \Delta \mathbf{x} + \frac{\partial (\mathbf{h}(\mathbf{x}))}{\partial \mathbf{u}}\Big|_{\mathbf{x}^B \mathbf{u}^B} \cdot \Delta \mathbf{u} \quad (12)$$

$$\mathbf{C}^B = \frac{\partial (\mathbf{h}(\mathbf{x}))}{\partial \mathbf{x}}\Big|_{\mathbf{x}^B}, \quad \mathbf{D} = \mathbf{0}. \quad (13)$$

Equations (11) and (13) will be discretized for each instant of time, yielding matrixes $\mathbf{A}_k$, $\mathbf{B}_k$ and $\mathbf{C}_k$. As we assume the output equation to be only dependent on $\mathbf{x}$, $\mathbf{D}_k$ will always be 0. With this, equations (5) and (6), which serve the purpose of determining the control actions of the predictive controller, can be easily constructed. The trajectory simulation is performed with the original nonlinear model from equation (4).

5. CASE STUDIES

To prove the applicability of the proposed combination of the LEM and LLT methods, two nonlinear SISO systems will be considered as example systems: a Van de Vusse reaction scheme and a heat exchange tank reactor.

5.1 Methodology and control objectives

The systems under consideration will be tested and compared in three different forms:

a) Nonlinear model. A nonlinear differential equation derived from first-principle modelling techniques. In this case the model will be assumed to represent the plant exactly. It is the best possible situation.

b) Analytic LEM model. A nonlinear LEM model is constructed by analytic calculation of the dynamic matrix **A** and the equilibrium manifold $\boldsymbol{\Omega}(u)$. The plant will be represented by the model used in *a).*

c) Interpolated LEM model. A nonlinear LEM model is constructed by spline interpolation of the dynamic matrix **A** and the equilibrium manifold $\boldsymbol{\Omega}(u)$ between different operating points. These operating points and their corresponding linear dynamics are to be determined analytically. The plant will be represented by the model used in *a).* As the analytic expressions for **A** and $\boldsymbol{\Omega}(u)$ will not be available in a real application of the LEM technique, this is a more realistic example.

For each of the mentioned models, numerical experiments with various LLT controllers in different operation domains are conducted. The controller parameters are determined using the RPN methodology developed by (Trierweiler and Farina, 2003), the control objective being a decrease of the closed-loop rise time to 1/6 of the open-loop rise time. For testing the closed-loop system, a series of random set point changes is applied to system controlled variable. Furthermore, the total cost J_{total} accumulated during the simulation time is compared, as well as the total necessary iterations.

5.2 The first example system: isothermal CTSR reactor with Van de Vusse reaction scheme

The Van de Vusse reaction scheme is a well-known benchmark problem for nonlinear control algorithms and has been studied extensively by various researchers. A detailed model for this system was presented in (Engell and Klatt, 1993). For shortness, only the differential equations will be shown here.

$$\begin{aligned} \dot{x}_1 &= -k_1 x_1 - k_3 x_1^2 + (x_{1,in} - x_1)u \\ \dot{x}_2 &= k_1 x_1 - k_2 x_2 - x_2 u \\ y &= x_2 \end{aligned} \quad (14)$$

In these equations x_1 is the concentration of component *A*, x_2 is the concentration of component *B* and $x_{1,in}$ is the feed concentration of *A*, assumed to remain constant. The parameter values are k_1=15.0345 h^{-1}, k_2 = 15.0345 h^{-1}, k_3 = 2.324 $l \cdot mol^{-1} \cdot h^{-1}$, $x_{1,in}$ = 5.1 $mol \cdot l^{-1}$ (Engell and Klatt, 1993). In this example only the operating range of $3 < u_s < 35$ h^{-1} is investigated.

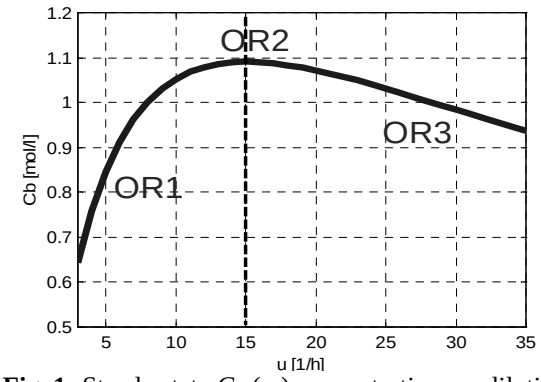

Fig. 1: Steady state C_B (x_2) concentration vs. dilution rate u for $x_{1,in}$ = 5.1 $mol \cdot l^{-1}$

A particularity of the Van de Vusse reaction is the division of the operating domain in two parts with different dynamic behaviours: Fig. 1 shows the steady state C_B solutions as a function of the dilution rate u with the three typical operating regions (i.e., OR1, OR2, and OR3). For OR1 (i.e., u_s < 15 h^{-1}) a non-minimum phase behaviour can be observed,

while for OR3 (i.e., u_s > 15 h^{-1}) the behaviour is minimum-phase. Close to peak the zero get close to origin, intensifying the non-minimum phase behaviour at the link side making the controller design more difficult. At the peak, the zero is null as well as the static gain, which is positive at OR1 and negative for OR3.

Numerical results. Details on obtaining the analytic and interpolated LEM systems will not be discussed here and can be found in Fernandes (2005). Note that the used spline interpolation of the equilibrium manifold and its associated dynamics are more exact for larger u_s.

First, OR1 and OR2 are investigated. In this region the proposed control goal could only be achieved by accepting excessive control action and large inverse responses. For this reason, the rise time will only be reduced to about 2/3 of the open-loop rise time. The following parameters are used for the LLT controller.

Table 1: non-minimum-phase LLT parameters

Prediction horizon (P)	68
Control horizon (M)	17
Output variable weight (Γ)	0.7
Input variable weight (Λ)	0.03
Sampling time (Ts)	0.3 min

The system is subjected to a series of setpoint changes in the region 0.7M < c_B < 1.11M.

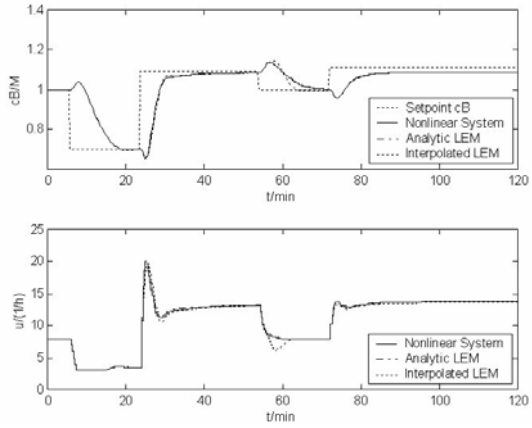

Fig. 2: time response in OR1 and OR2

In the first 20 minutes of the simulation, the closed-loop velocity is limited by the lower constraint of u = $3h^{-1}$. The next setpoint is c_B=1.09M which is the theoretical maximum of the concentration c_B (OR2, cf. Fig. 1). Up to this point, the behaviour of nonlinear system, analytic LEM and interpolated LEM is very similar. Note that the LEM step response behaviour is comparable to the behaviour of the corresponding linear model *at the new setpoint* (Fernandes 2005). Around the 60th minute, the first major deviation of the interpolated LEM occurs because of a difference between the interpolated and the exact equilibrium manifold around u = $7.96h^{-1}$.and c_B = 1M. From the 75th minute, the system is subjected to a setpoint of c_B = $1.11h^{-1}$ that is not attainable (see Fig. 1). With all three model versions, the controller stabilizes the system at the maximum value of c_B = $1.09h^{-1}$. This is a clear advantage in comparison to a linear (e.g. PI) controller which would not be able to keep the system at the point of maximum yield.

Now the region OR3 for 1M < c_B < 1.09M is investigated. Minimum-phase behaviour causes a better overall performance. First, the controller shown above is tested in the minimum-phase region with a series of setpoint changes of random magnitude to prove the usability of one set of control parameters for the whole operation domain. Fig. 3 shows these results for OR3, while Fig. 4 shows the same setpoint changes applied to OR1.

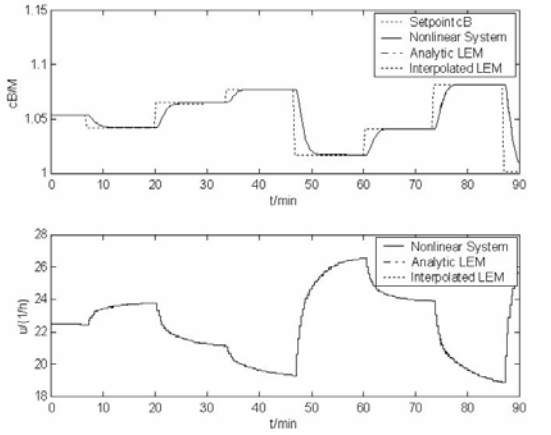

Fig. 3: minimum-phase responses, 1M < c_B < 1.09M.

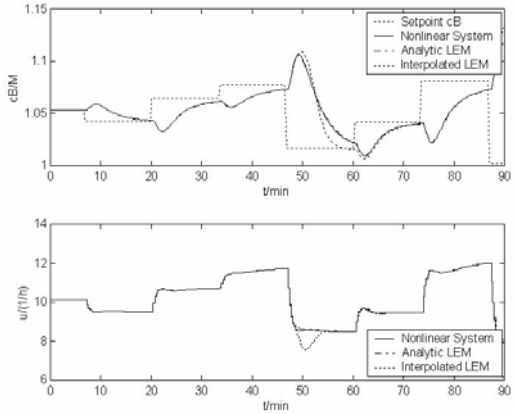

Fig. 4: non-minimum-phase responses, 1M < c_B < 1.09M

Table 3: minimum-phase and non-minimum-phase performance, 1M < c_B < 1.09M

	Nonlinear	Analytic	Interpolated
Iterations, min.-phase	418	418	419
J_{total}, m.p.	0.2830	0.2832	0.2840
Iterations, n.-min.-phase	353	353	363
J_{total}, n.m.p.	5.0712	5.1753	4.5228

Finally, a controller designed especially for the minimum-phase region will be tested to see how the performance can be improved, when the right tuning parameters are applied. Table 3 summarizes the new controller parameters.

Table 3: minimum-phase LLT parameters

Prediction horizon (P)	14
Control horizon (M)	4
Output variable weight (Γ)	0.7
Input variable weight (Λ)	0.003
Sampling time (Ts)	0.3 min

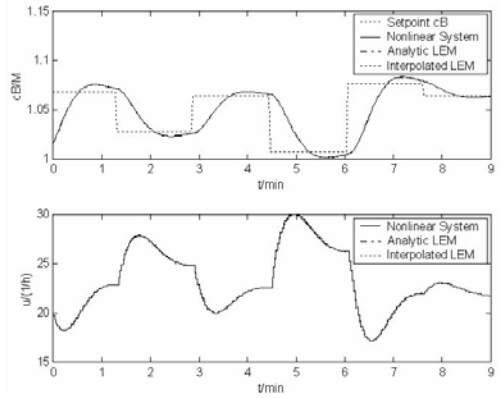

Fig. 5: minimum-phase responses, faster controller

It is evident that this controller performs much better than the one designed for non-minimum-phase behaviour, which makes it the preferable option for operation near the maximum yield of c_B=1.09M. However, it has to be assured that the system does not trespass into the non-minimum-phase region, since in this case it would cause excessive inverse responses. This can be achieved by defining a 'target' for the manipulated variable in the minimum-phase domain within the LLT algorithm.

Table 4: minimum-phase performance, $1M < c_B < 1.09M$

	Nonlinear	Analytic	Interpolated
Iterations	993	994	993
J_{total}	1.5177	1.4986	1.5195

As expected, the analytic LEM model performs well in all the shown cases with only slight deviations from the original nonlinear model. The performance losses of the interpolated LEM model occur because of the error in the interpolation.

5.1 The second example system: heat exchange tank reactor

The heat exchange tank reactor consists of an adiabatic tank containing three chambers whose dividing walls are impermeable for mass and only permit heat exchange. The three chambers are positioned in a way that only the central chamber is in contact with the two others and exchanges heat with the hot (h) and cold (c) chamber. The three chambers have constant volumes V_c, V and V_h and distinct feed flows with water at different temperatures T_{ci}, T_i and T_{hi} respectively. The two dividing walls in the tank have global heat transfer coefficients U_c, U_h corresponding to the divisions between $V_c|V$ and $V_h|V$. The existing heat transfer causes a variation in the chambers' outflow temperatures T_c, T and T_h. In this case, the system is regarded as SISO. The manipulated variable is the feed flow F_{ih}, the controlled variable the temperature T.

The differential equations are as follows:

$$\begin{aligned}
\frac{dT_h}{dt} &= \frac{F_{hi}\cdot(T_{hi}-T_h)}{V_h} - \frac{U_h\cdot A_h}{V_h\cdot Cp_h\cdot\rho_h}(T_h-T)\\
\frac{dT_c}{dt} &= \frac{F_{ci}\cdot(T_{ci}-T_c)}{V_c} - \frac{U_c\cdot A_c}{V_c\cdot Cp_c\cdot\rho_c}(T_c-T)\\
\frac{dT}{dt} &= \frac{F_i\cdot(T_i-T)}{V} + \frac{U_h\cdot A_h}{V\cdot Cp\cdot\rho}(T_h-T) + \frac{U_c\cdot A_c}{V\cdot Cp\cdot\rho}(T_c-T)
\end{aligned} \qquad (15)$$

The following set of parameters is used for the experiments: ρ = 1000 kg/m^3; Cp = 4180 J/kg/K; V = 3 m^3; ρ_c = 1000; Cp_c = 4180 J/kg/K; V_c = 3 m^3; ρ_h = 1000 kg/m^3; Cp_h = 4180 J/kg/K; V_h = 3 m^3; $U_h \cdot A_h$ = 300 J/K/s; $U_c \cdot A_c$ = 100F_{hi} J/K/s; F_{ci} = 0 m^3/s; F_i = 0.001 m^3/s; T_{hi} = 370 K; T_{ci} = 280 K; T_i = 300 K. Controller design was performed at the point of operation F_{hi} = 0.0013* m^3/s; $T_h = T_c$ = 339.80 K; T = 339.25 K .

Numerical results. The tank reactor shows minimum-phase behaviour in the whole operation domain. Note that the time response to a positive perturbation in open loop is about three times faster than the time response to a negative perturbation. The interpolation of the equilibrium manifold is done by using 4th-order splines. The matrix **A** used for construction of the LEM is linear in u, for this reason the analytic and interpolated versions are the same.

Two areas of operation will be investigated: the lower region of $300K < F_{hi} < 339.25K$, and the upper region of $339.25K < F_{hi} < 365K$ where the system response to variations in F_{hi} is rather small. The controller parameters are as follows:

Table 5: Tank reactor LLT parameters

Prediction horizon (P)	26
Control horizon (M)	7
Output variable weight (Γ)	0.7071
Input variable weight (Λ)	5.2129
Sampling time (Ts)	20s

As shown below, the system shows good control performance in the upper operation region.

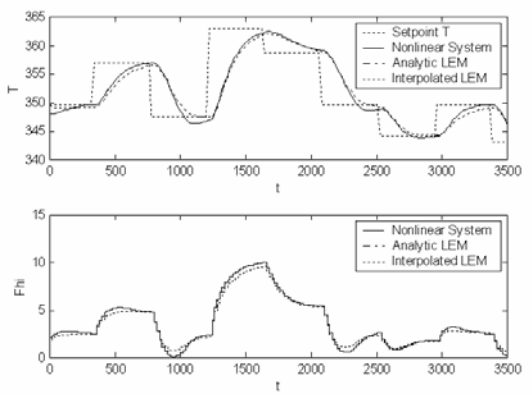

Fig. 6: time response for upper region

Table 6: performance in upper region

	Nonlinear	Analytic	Interpolated
Iterations	212	212	206
J_{total}	$1.888 \cdot 10^4$	$1.888 \cdot 10^4$	$1.716 \cdot 10^4$

In the lower region, the effect of slower responses with negative setpoint changes is more visible. However, all three models show a quite similar behaviour.

Table 7: performance in lower region

	Nonlinear	Analytic	Interpolated
Iterations	188	188	188
J_{total}	$1.131 \cdot 10^5$	$1.131 \cdot 10^5$	$1.502 \cdot 10^5$

The plot shows that this system can be controlled with good performance with the LEM+LLT combination.

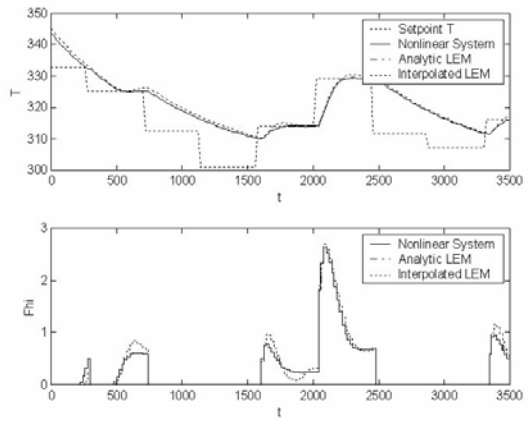

Fig. 6: time response for upper region

6. CONCLUSIONS AND OUTLOOK

In this paper the proposal for a combined use of the nonlinear modelling and identification technique LEM and the nonlinear predictive control algorithm LLT was made and tested with two SISO examples. Analytical considerations and numerical results suggest a good applicability of this combination to lower order SISO systems. Losses in control performance are mainly due to the inevitable deviation of the interpolated equilibrium manifold and the associated dynamics from the true nonlinear system's dynamics. The necessary iterations for convergence of the algorithm, as well as the accumulated values of the objective function are in all cases in the same scale, they can vary slightly because of the described deviations. It is clear that large efforts have to be made to obtain good approximations for the equilibrium manifold and the associated dynamics. Taking this into account, it can be concluded that further investigation of the demonstrated combination appears promising. Future work will be done on the testing of the technique with MIMO models and models of higher order, the goal being the proof of applicability to real industrial processes. The second possibility of implementation mentioned in section 4, the alteration of the LLT algorithm to be directly suitable for the LEM structure, will also be explored.

REFERENCES

Duraiski, R.. G.; (2001a) Controle Preditivo Não Linear Utilizando Linearizações ao Longo da Trajetória; M. Sc. Thesis, UFRGS, Brazil.

Engell, S. and K. U. Klatt (1993). Nonlinear Control of a Non-Minimum-Phase CSTR. *Proceedings of the American Control Conference*, pp. 2041-2045, San Francisco, California, June 1993.

Bolognese Fernandes, P. (2005). *The input-parameterized linearization around the equilibrium manifold approach to modeling and identification*. Phd Thesis, University of Dortmund (to be published).

Bolognese Fernandes, P., S. Engell (2005). Continuous Nonlinear SISO System Identification using Parameterized Linearization Families. *Proc. of the XVI IFAC World Congress, Prague, Tchech Republic*.

Johansen, T.A. and R. Murray-Smith (1997). The Operating Regime Approach to Nonlinear Modelling and Control. *Multiple Model Approaches to Nonlinear Modelling and Control* (R. Murray-Smith and T.A. Johansen. (Eds)), pp. 3-72. Taylor & Francis, London.

Nelles, O. (1997). LOLIMOT- Lokale, lineare Modelle zur Identifikation nicht-linearer, dynamischer Systeme. *Automatisierungstechnik*, **4**, 163-174.

Trierweiler, J. O., Farina, L. A. (2003), RPN tuning strategy for model predictive control. *Journal of Process Control*, v. 13, p. 591-598, 2003.

Wang, J. and J. W. Rugh (1987). Parameterized Linear Systems and Linearization Families for Nonlinear Systems. *IEEE Transactions on Circuits and Systems*, **34**, 650-657.